ALK-EML4-Positive Cancers and Combination Therapy: Probing the Apoptotic Threshold

Undergraduate Thesis
10 April 2018

University of Colorado – Boulder
Department of Chemistry & Biochemistry

TABLE OF CONTENTS

Abstract

Of all diseases currently being researched, lung cancer is one of the most pressing due to its worldwide prevalence and high incidence of fatality. More specifically, non-small cell lung cancers (NSCLC) harboring ALK-EML4 gene fusion mutations are of particular interest to researchers due to their widely documented capability of becoming resistant to specialized treatment, such as kinase inhibition. This project was initiated with the aim of using *in vitro* combination drug treatment to more efficaciously inhibit the growth and survival of H3122 cells, an ALK-EML4-positive NSCLC cell line. In this study, H3122 cells were subjected to combined ALK and histone deacetylase (HDAC) inhibition; two ALK inhibitors, crizotinib and AP23116, were combined with paragazole, a class-1 HDAC inhibitor. Both combinations, crizotinib/paragazole and AP23116/paragazole, were found to produce lower EC_{50} values than single-drug treatment. While each drug pair confers synergistic activity, the latter combination was found to be substantially more potent. ALK and HDAC inhibition in combination proves to be an effective means of treating ALK-EML4-positive cells and could be a successful approach to counteracting acquired drug resistance in cancers with ALK rearrangements.

Introduction

Globally, lung cancer is one of the most common, as well as fatal forms of cancer. Specifically, non-small cell lung cancer (NSCLC) is the most prevalent form, constituting 4 in 5 lung cancer diagnoses (American Cancer Society). While many people who are diagnosed with NSCLC undergo successful treatment, whether it is general cytotoxic chemotherapy or targeted treatment, certain mutations can arise in these cancers that undermine the efficacy of current therapeutics. First identified in 2007, the gene fusion product of ALK (anaplastic lymphoma kinase) and EML4 (echinoderm microtubule-associated protein-like 4) was the first ALK rearrangement found in non-small cell lung cancers (Soda et al. 2007). While over 20 ALK fusion partners have been identified, EML4 is one of the most common, constituting 29-33% of ALK-positive diagnoses (Chiarle et. al 2008; Chia et al. 2014). Currently, there are several drugs that specifically inhibit the kinase activity of ALK, with crizotinib being the most popular among clinical trials. While ALK-inhibition treatment initially causes tumors to regress and patient health to improve, no case has been documented in which the cancer does not relapse within one year (Takezawa et. al 2011).

The individual genes of the fusion product have known functions: ALK has been found to play a role in regulating the development of the embryonic nervous system, but researchers have not successfully found endogenous activating ligands (Bayliss et. al 2016). EML4 functions as a regulator of α- and β-tubulin polymerization and degradation (Chia et al. 2014). However, the fusion product has entirely different characteristics of expression and down-stream regulation. Several variants of the fusion have been identified, all of which contain the complete ALK gene, comprised of exons 20-29 (Sasaki et al. 2010). The difference between the variants of ALK-EML4 (v1, v2, v3a, v3b, v4a, v4b, v5a, and v5b) is

the portion of EML4 to which ALK is fused (Heuckmann 2012). All variants respond to ALK inhibition (ALKi), albeit with varying differing sensitivities. Independent of the particular variant, all ALK-EML4 fusion products demonstrate oligomerization, yielding constitutive kinase activation. Growth and proliferation of cells harboring ALK-EML4 decrease markedly in response to ALK inhibition, conferring oncogenic addiction to the gene fusion. No matter the degree of sensitivity of the ALK-EML4 variant to ALK inhibition treatment, clinical studies report that all patients inevitably relapse within 12 months of treatment, which is a clear indication of acquired drug resistance (Sasaki et al. 2010). The ability of ALK-EML4 to evade ALKi-induced apoptosis depends upon important survival pathways – namely ERK (extracellular-regulated kinase) and STAT3 (signal transducer and activator of transcription 3) (Katayama et al. 2011). ERK and STAT3 regulate the production of key apoptotic factors, such as Bim, a pro-apoptotic protein of the Bcl-2 family, and survivin, an anti-apoptotic protein. Takezawa et al. present striking evidence that when the ALK gene is silenced, the phosphorylation of ERK and STAT3 becomes markedly abrogated. Not only were these phosphorylated proteins screened for, but their apoptosis-regulating products, Bim and survivin, were assayed for as well. It was found that when treated with an ALK inhibitor, TAE684, Bim was massively up-regulated, while survivin was down-regulated. ALK induction activates ERK and STAT3, while ALK inhibition increases pro-apoptotic factors and decreases pro-survival factors, indicating that ALK-EML4 cancers rely heavily upon the ERK and STAT3 pathways to trigger essential survival and proliferative processes.

While next-generation ALK inhibitors are being developed that have different mechanisms than crizotinib, many researchers are employing combination therapy in an effort to overcome acquired resistance to ALK inhibition. Groups have reported success in overcoming resistance in various ALK+ cancers using *in vitro* treatment of combinations of

crizotinib and MDM2 inhibitors and crizotinib and Hsp90 inhibitors (Wang et al. 2017; Sang et al. 2013). Despite the fact that MDM2 and Hsp90 inhibitors have very different targets and modes of actions, when in combination with crizotinib, these treatments yielded appreciable loss of phosphorylated ALK and ERK. Clearly, the approach of combinatorial treatment is both valid and promising, since multiple groups have reported combinations that induce apoptosis and cell-cycle arrest more effectively than ALKi treatment on its own.

In this study, I evaluated the treatment of H3122 with two ALK inhibitors (crizotinib and AP26113) when combined with paragazole, an HDAC inhibitor. H3122 is a non-small cell lung cancer cell line that harbors ALK-EML4 variant 1, which has been found to be the most sensitive variant to ALKi (Yoshida et al. 2016). Crizotinib is an ATP analog that competitively binds the ALK kinase domain. AP26113 is a next-generation ALK inhibitor with a structure and binding mechanism that confers more selective inhibition (Zhang et al. 2016). Paragazole is a class I HDAC inhibitor that preferentially inhibits the activity of HDAC1, 2, 3, and 8, all of which are localized in the nucleus. HDAC inhibition (HDACi) has been found to reduce tumor progression in a variety of cancers by inducing apoptosis via p53-dependent and independent pathways, as well as inducing cell-cycle arrest (Li et al. 2014). By first establishing the dose-responses of H3122 to single drug treatments with crizotinib, AP21136, and paragazole, the effects of combination treatment could be more definitively analyzed. Our lab was fortunate enough to have collaborated with Dr. Anang Shelat and Dr. Nathaniel Twarog of St. Jude Children's Research Hospital, who formulated and developed the Bivariate Response to Additive Interacting Doses (BRAID) analysis, a tool specifically designed to quantify synergistic effects of drug combinations. This analysis utilizes the measurements of maximal efficacy, potency, and Hill equation parameters

(sigmoidicity of dose-response) of each drug to produce an effect as a function of two doses (Twarog et al. 2016). I also employed analytical tools such as EC_{50} analysis and GraphPad Prism to verify that the combination of ALK and HDAC inhibition indeed produces a synergistic effect. By using various analytical techniques, including BRAID analysis, I found that combination ALKi/HDACi treatment is more efficacious than single-drug treatment.

Materials & Methods

Cell lines and Culture

The H3122 NSCLC cells were cultured in RPMI 1640 medium supplemented with 10% FBS, 0.2 mM L-glutamine, 10 units/mL Penicillin G sodium, and 10 μg/mL Streptomycin sulfate. H3122s were passaged every 3-5 days and replenished with fresh media every 72 hours. H3122 samples were found to be mycoplasma-free via flow cytometry screening.

Drug Reagents

The therapeutic agents used throughout this project were two ALK inhibitors (crizotinib and AP23116) and paragazole, a class-I HDAC inhibitor.

Crizotinib:

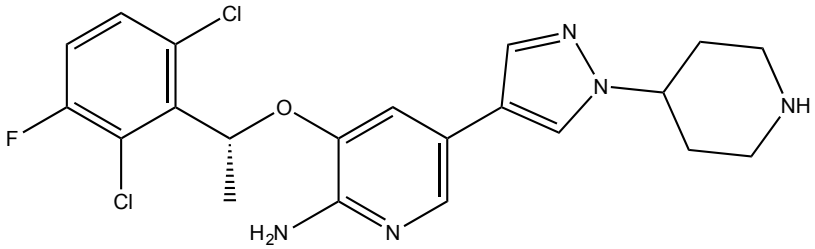

AP23116:

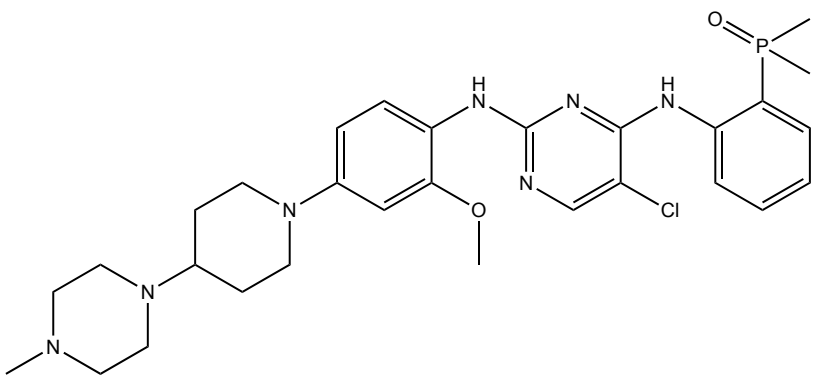

Paragazole:

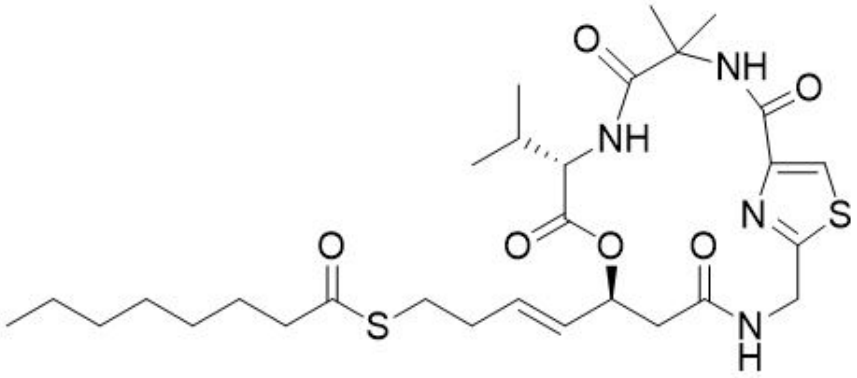

Single-Drug and Simple Combination Dose-Response Treatments

Cells were seeded in Eppendorf 96-well plates with a built-in reservoir to reduce the edge effect and evaporation overall. Each plate was seeded with 1/8 of a 70-80% confluent 15 cm^2 culture dish, ~ 20,000 cells per well. Cells were allowed to culture and adhere to the plate for 48 hours. Drug reagents were then added at concentrations ranging from 2.4-9.6 μM and serially diluted across the plate (two-fold dilutions). Drug combinations were added at equal concentrations and various other ratios. The last two columns (16 wells)

were treated with DMSO as positive controls. The cells were cultured for 4 days after drug treatment, before being fixed and stained for viability.

BRAID Combination Treatments

The BRAID analysis called for an 8 96-well plate set-up for each combination (crizotinib/paragazole and AP23116/paragazole). In order to produce the parameters necessary for successful analysis, H3122s were treated with each compound in combination with itself and DMSO, in addition to the combination of the two drugs. Two compounds were added to each plate at concentrations of 9.6 μM, with one added and diluted (two-fold) in the landscape orientation and the other added and diluted (two-fold) in the portrait orientation (refer to schematic below). Treatments with drugs in combination and with a single drug in combination with DMSO were done in each possible orientation, resulting in two combination trials, two single drug/DMSO trials for each compound, and one self-self combination for each drug. Cells were then fixed with para-formaldehyde and stained with crystal violet. Once obtained, raw absorbance data was sent to Dr. Anang Shelat and Dr. Nathaniel Twarog to be analyzed using the BRAID algorithm.

BRAID Set-up

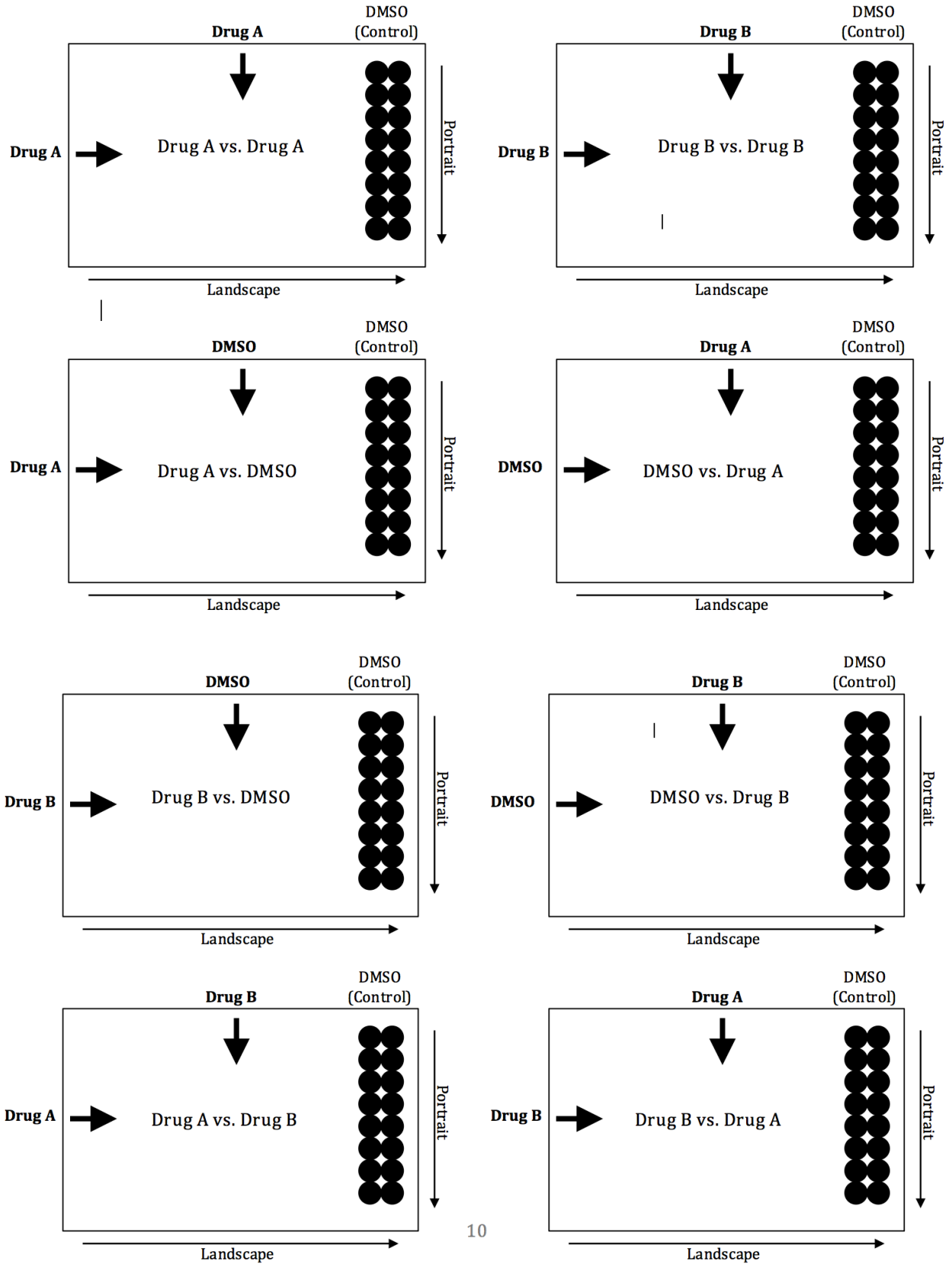

10

Staggered Combination Treatments

H3122 cells were seeded at ~20,000 cells/well on Eppendorf 96-well plates and allowed to culture and adhere for 24 hours. Cells were treated with the same combinations as before: AP23116/paragazole and crizotinib/paragazole. For each combination, AP23116 or crizotinib was added at 1.2 μM and diluted across the plate (two-fold dilutions). 24 hours after ALKi treatment, paragazole was added at 1.2 μM and diluted across the plate (two-fold dilutions). Trials were also conducted with paragazole as the initial treatment (1.2 μM) and either AP23116 or crizotinib (1.2 μM) was added 24 hours after addition of paragazole. Cells were fixed and stained for viability 72 hours after the addition of the second drug. Results are the averages of two biological replicates of each combination in each permutation.

Cell Fixation & Viability Assays

After treatment, cells were fixed to plates using either 4% para-formaldehyde/H_2O solution or cold methanol fixation. For para-formaldehyde fixation, cells were first rinsed with PBS then treated with para-formaldehyde for six minutes. The para-formaldehyde was then discarded from the microplate and cells were then treated with crystal violet for 8 minutes and gently rinsed with cold water. Cold methanol was employed after a consistent loss of cells was observed during the para-formaldehyde fixation process. This fixation protocol entailed filling the microplate with -20°C methanol and allowing to equilibrate at -20°C for 15 minutes. The methanol was then discarded and the microplate was rinsed with room temperature PBS three times. Cells were then treated with a 0.05% crystal violet/methanol/H_2O solution for 8 minutes (200 μL/well), and then gently rinsed with cold water. Plates were allowed to dry for 24 hours. Visualizing agent (4:1:1 H_2O/methanol/ethanol) was then added to the plate (160 μL/well) and plates were left to

equilibrate for 1 hour at 0°C. All plates were scanned using either a Tecan or Perkin Elmer microplate reader. Absorbance was measured as 530 nm with a reference wavelength of 0 nm.

Data Analysis

The first step upon obtaining raw absorbance data was to normalize experimental values as a fraction of the average of all DMSO-treated wells (positive control). This established the average absorbance of positive controls as the maximum value. Then, averages were taken between identically treated wells, since at least two rows of cells were given the same drug concentrations. Since the absorbance values are indicative of the alive, or unaffected population, these values were subtracted from 1 in order to achieve the fraction of cells affected by treatment. Averages were then taken among biological replicates and fit with standard error bars. Dose-response data was then fit with sigmoid curves and EC_{50} values were determined with GraphPad Prism.

Results

Single-Drug Treatments

In order to establish a base line for combination treatments, the response of H3122 cells to each of the therapeutic compounds was determined. Averages were taken from four biological replicates of treatments with each drug: crizotinib, AP26113, and paragazole. For crizotinib, the EC_{50} was determined to be 0.97 μM (*Fig. 1A*). This result is concurrent with another group that established an IC_{50} of 1 μM (Katayama et al. 2012). AP26113 exhibited a higher potency, with an IC_{50} of 0.40 μM (*Fig. 1B*). It is apparent when the curves of the two ALK inhibitors are overlaid that crizotinib produced inferior effects (*Fig. 1C*). The dose-

response curve of AP23116 demonstrates a steeper initial slope of the curve and a larger effect at the same concentrations as crizotinib, indicating higher biological activity and maximal efficacy. Paragazole exhibited the least potency, by far, with an EC_{50} of 3.5 μM (*Fig. 1D)*. Perhaps the most striking characteristics of paragazole treatment compared to that of treatment with either ALK inhibitor is the relatively miniscule slope and maximal efficacy of the dose-response. While higher concentrations of paragazole would be necessary to achieve a complete sigmoidal dose-response, the data collected represents the relative ineffectiveness of HDACi on its own. Based on the data produced from single-drug treatments, it is evident that both crizotinib and AP23116 on their own achieve powerful maximal efficacies, as well as potencies at reasonable concentrations, in terms of short-term *in vitro* treatment. Paragazole, on the other hand, exhibits minimal potency and maximal efficacy, even at concentrations much larger than that of either ALK inhibitor. Clearly, it is the kinase activity of the ALK-EML4 fusion protein that predominantly confers survival. Due to the disparity between the effects of individual HDAC and ALK inhibition, it is not obvious that much stronger activity would be achieved in response to treatment with paragazole in combination of each of the two ALK inhibitors.

Figure 1. *Single-drug dose-responses. (A) Dose-response of H3122 to crizotinib. (B) Dose-response of H3122 to AP21136. (C) Overlay of dose-response of H3122 to crizotinib (blue) & AP23116 (green); arrows indicate location of* EC_{50}*. (D) Dose-response of H3122 to paragazole.*

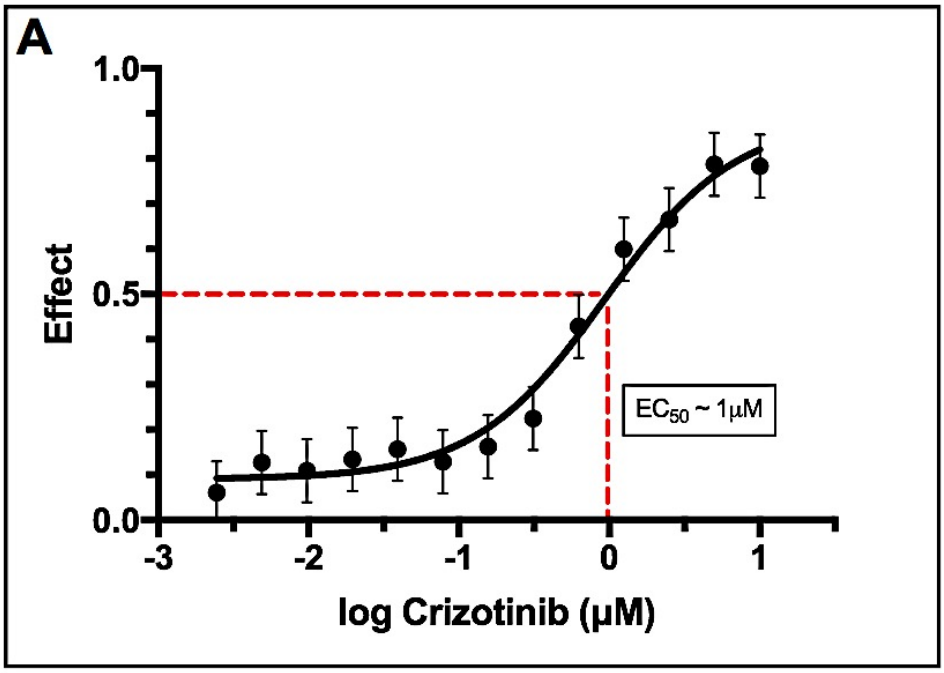

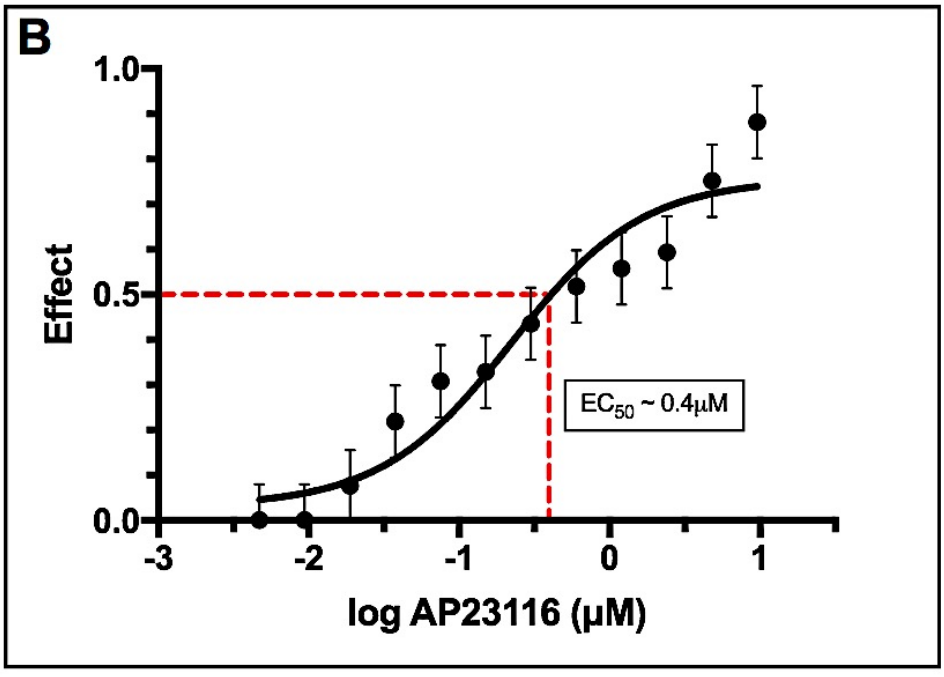

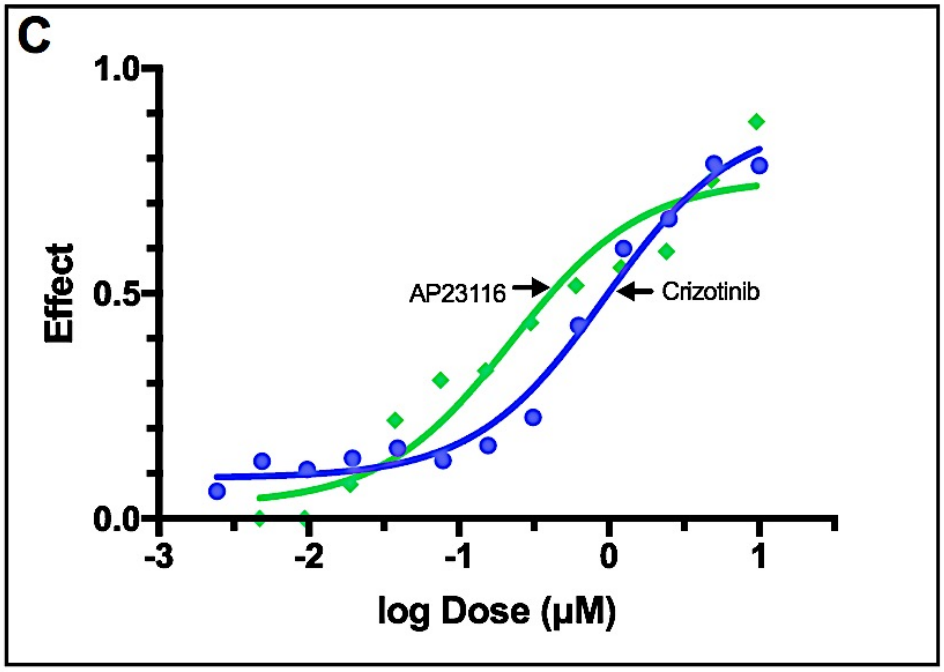
C
1.0
0.5
0.0
Effect
AP23116
Crizotinib
-3
-2
-1
0
1
log Dose (μM)

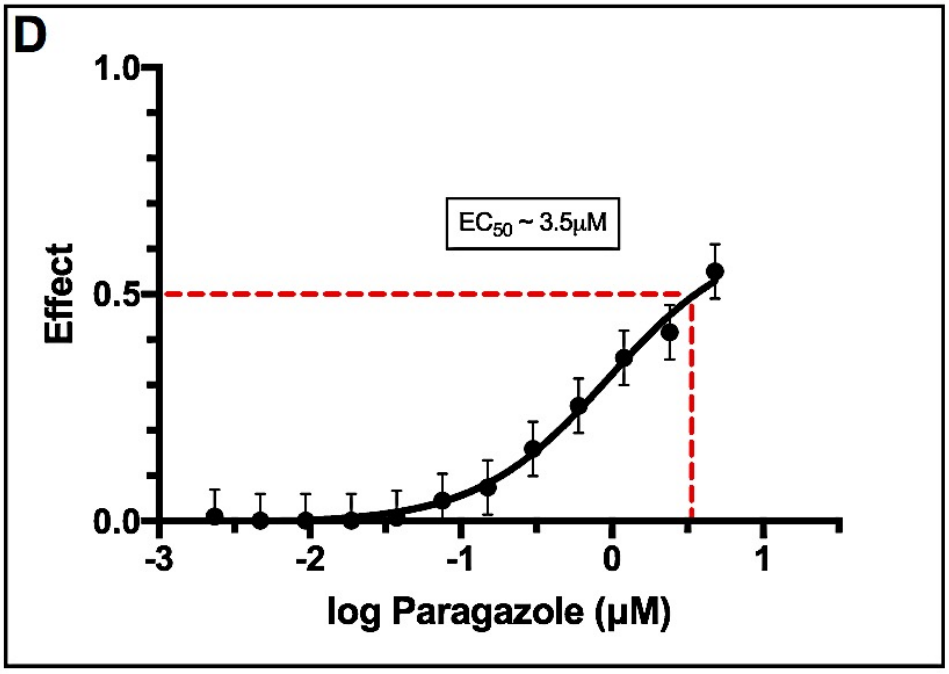
D
1.0
0.5
0.0
Effect
EC50 ~ 3.5μM
-3
-2
-1
0
1
log Paragazole (μM)

Combination BRAID Treatments

The focus of BRAID analysis is being able to quantify synergistic activity between two drugs in combination by creating a response surface model. Drug relationships are represented and evaluated by the κ value, where $\kappa<0$, $\kappa=0$, and $\kappa>0$ are indicative of antagonism, additivity, and synergism, respectively. A crucial element of the experiment is establishing the baseline activity of each individual drug. This was done by treating H3122 with crizotinib, AP23116, and paragazole "in combination" with themselves in order to achieve purely additive responses. These self-self combinations yielded κ values very close to zero (*Fig. 2*). The slight deviation of these values from $\kappa=0$ is not indicative of antagonism, in the case of ALK self-self trial, or synergism, in the case of the HDAC self-self trial, but rather demonstrates that the set-up for the experiment was less than perfect; the numerous intensive and tedious steps of the drug addition process for BRAID analysis yield many opportunities for small errors to be made. The presented data were produced from two biological replicated of each combination.

Establishing an additive baseline with the self-self trials is necessary to accurately determine the relationship between ALK and HDAC inhibitors when H3122s were treated with the two combinations: crizotinib/paragazole and AP23116/paragazole. In order to verify the combination response, each drug pair is tested on two microplates, with the two drugs added in two different orientations. For each combination, crizotinib/paragazole and AP23116/paragazole, κ values of well over zero were produced, indicating strong synergistic activity for each ALKi/HDACi pair (*Fig. 3*). Not only do the κ values confer synergy, but so do the response surfaces produced by the BRAID analysis (*Fig. 4)*. The key feature of a synergistic surface response is the rounding of the response as the concentrations of each drug increase. This is clearly seen in both the crizotinib/paragazole

(*Fig. 4A)* and AP23116/paragazole (*Fig. 4B)* response surfaces. This rounding indicates that as the concentration of one drug increases, less and less of the other drug is required to produce the same effect, exemplifying a synergistic relationship between each ALK inhibitor and paragazole. All results yielded positive κ values, yet with varying magnitudes due to imperfect drug additions. While BRAID analysis is indeed a powerful tool, it is difficult to obtain clean results since such a large number of parameters must be addressed. Imperfect drug addition caused variability in responses for each drug. Synergistic activity was observed in all trials of both ALKi/HDACi combinations, but due to the complicated nature of the set-up, we decided to move towards more straightforward combination treatments that would allow more definitive results to be obtained.

Figure 2. *BRAID results for self-self crosses*

Drug Combinations	**κ Values**
AP23116 vs. AP23116	-1.02
Crizotinib vs. crizotinib	-0.42
Paragazole vs. paragazole	0.32

Figure 3. *BRAID results for combination crosses*

Drug Combinations	**κ Values**
AP23116 vs. Paragazole (Orientation 1)	100
Paragazole vs. AP23116 (Orientation 2)	100
Crizotinib vs. Paragazole (Orientation 1)	100
Crizotinib vs. Paragazole (Orientation 2)	100

Figure 4. *BRAID response surfaces for combination trials. HDACi concentration is plotted on the x-axis; ALKi concentration is plotted on the y-axis. (A) Crizotinib vs. paragazole. (B) AP23116 vs. paragazole.*

A

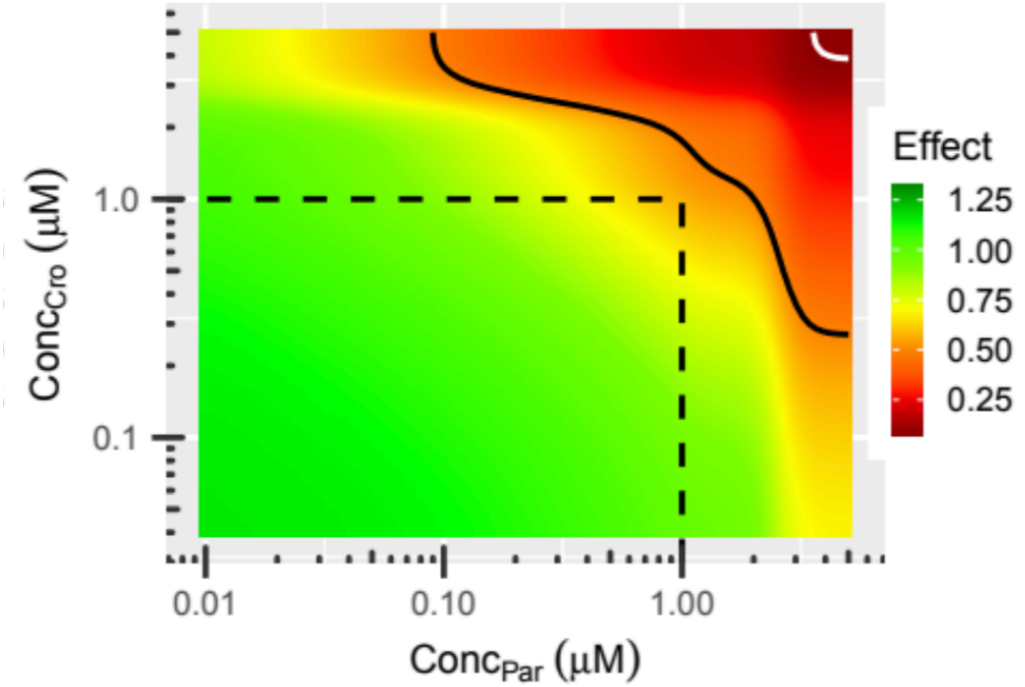

B

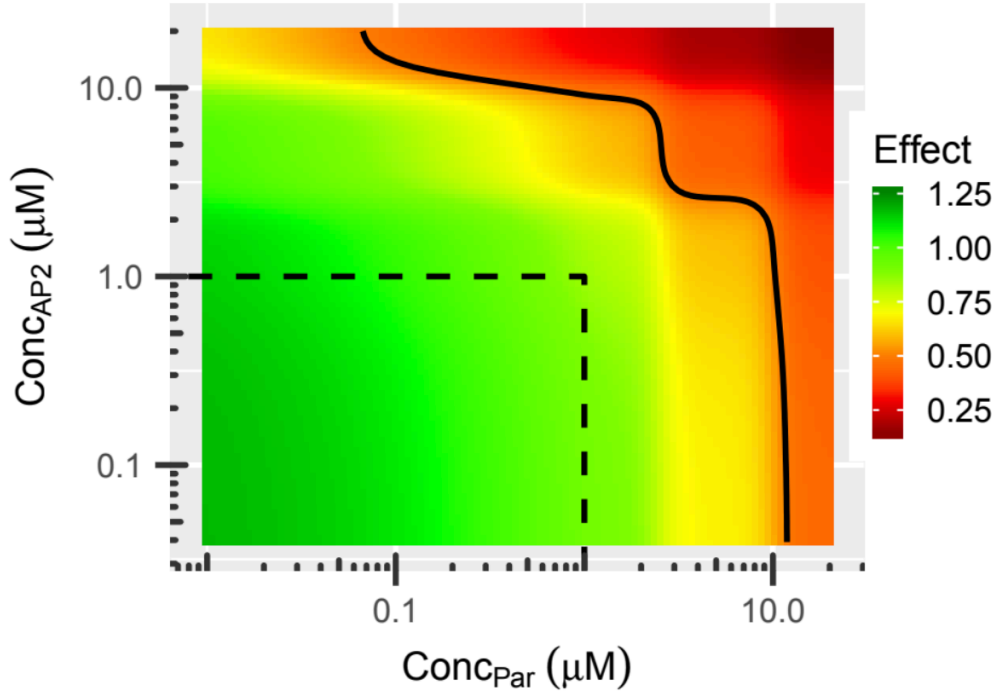

Simple Combination Treatments

For these combination treatments, results were obtained from four biological replicates of experiments in which H3122 cells were treated with either the crizotinib/paragazole or AP23116/paragazole combination. Cells were treated with combinations ranging from 0.1-9.6 μM in order to achieve complete dose-responses. While both ALK inhibitors and paragazole were sampled in varying ratios to each other, the presented results are of 1:1 ALK/paragazole treatments. When H3122s were treated with crizotinib in combination with paragazole, the observed EC_{50} was 0.7 μM (concentration of each drug) (*Fig. 5A)*. In terms of synergy, the combination is not drastically more effective than crizotinib on its own (EC_{50} 0.97 μM). However, when compared to crizotinib by itself, crizotinib and paragazole in combination do exhibit a higher potency and biological activity (steeper slope), as well as higher maximal efficacy (*Fig. 5C)*.

The combination of AP23116 and paragazole, on the other hand, exhibited marked effectiveness, with an EC_{50} of 0.04 μM (*Fig. 5B)*. When overlaid with single-drug AP23116 treatment, the dose-response of combination treatment is indicative of substantially higher biological activity and potency (Fig. 5D). The EC_{50} of the combination is more than ten-fold less than that of AP23116 alone (0.04 μM vs. 0.6 μM, respectively). Clearly, H3122 cells are vastly more sensitive to the combined action of AP23116 and paragazole than any single-drug treatment. Something to note is the irregular shape of the dose-response curve of the AP23116/paragazole combination; while all other treatments can be closely fit with normal sigmoidal response curves, this combination exhibits a parabolic dose-response (*Fig. 5B)*. Among all four biological replicates, there were no significant outliers or irregularities, leading me to believe that this dose-response is valid. This shape is indeed irregular, but the steepness of the curve is due to substantial effects at very low

concentrations of AP23116 and paragazole, emphasizing the efficacy of the combination. AP23116 exhibits an EC_{50} of more than two-fold less than crizotinib, yet when combined with paragazole, the AP23116 produces a much larger-fold increase in efficacy. Evidently, potent ALK inhibition sensitizes H3122s to HDAC inhibition to a greater extent.

Figure 5. *Simple combination treatments; dosage represents the concentration of each drug in combination. (A) Dose-response of H3122 to crizotinib & paragazole in combination. (B) Dose-response of H3122 to AP23116 & paragazole in combination. (C) Overlay of dose-responses of H3122 to crizotinib (blue) and crizotinib & paragazole in combination (purple); arrows indicate EC_{50} concentration. (D) Overlay of dose-responses of H3122 to AP23116 (green) and AP23116 & paragazole in combination (red); arrows indicate EC_{50} concentration. (E) Overlay of dose-responses of H3122 to crizotinib & paragazole in combination (purple) and AP23116 & paragazole in combination (red); arrows indicate EC_{50} concentration.*

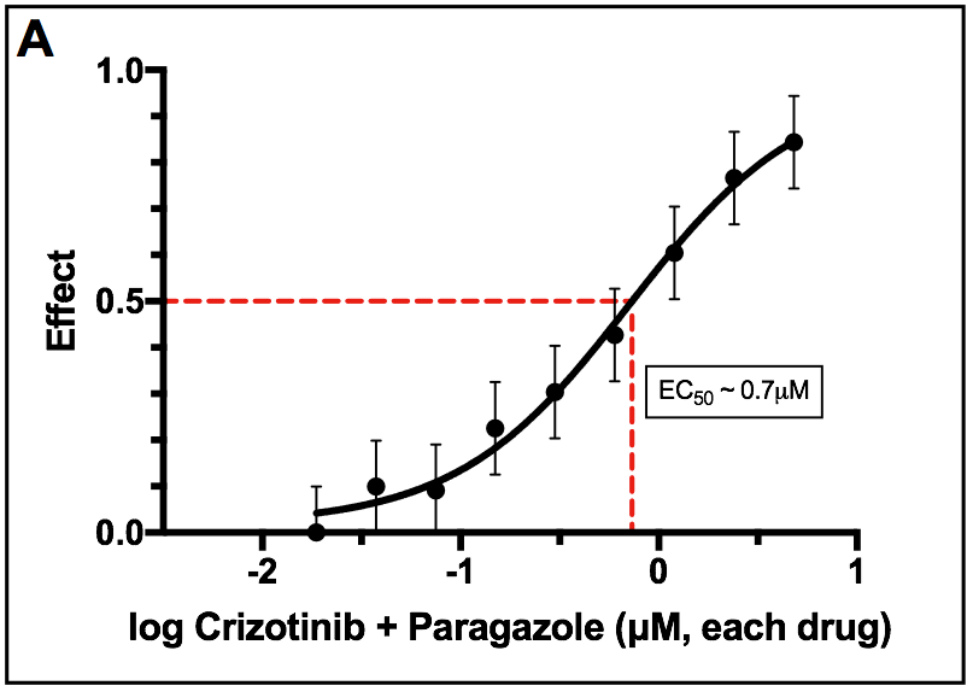

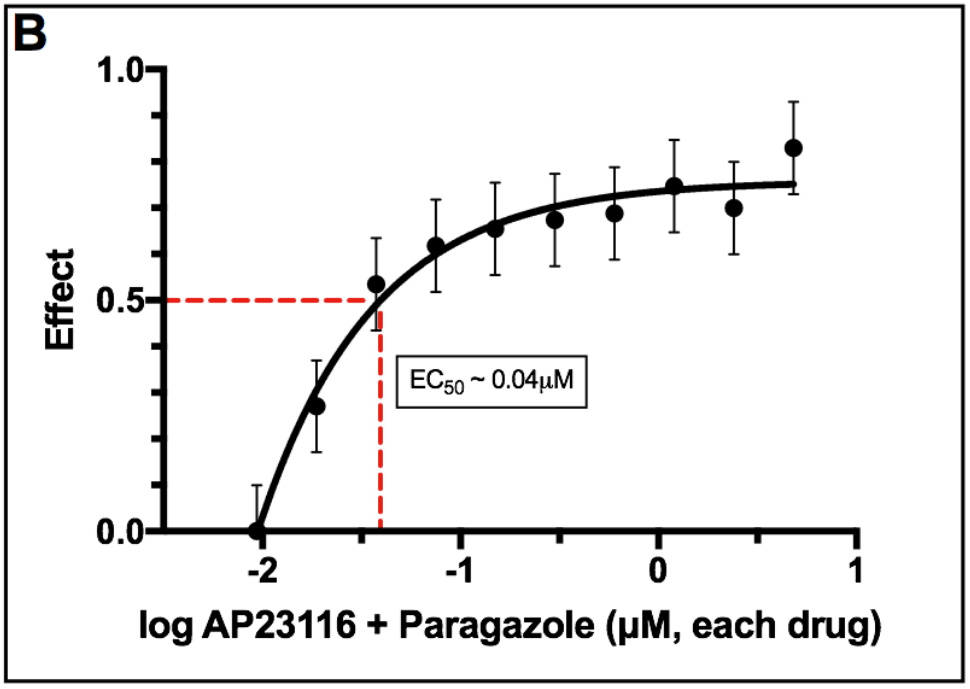
B
1.0
0.5
0.0
Effect
EC50 ~ 0.04μM
-2
-1
0
1
log AP23116 + Paragazole (μM, each drug)

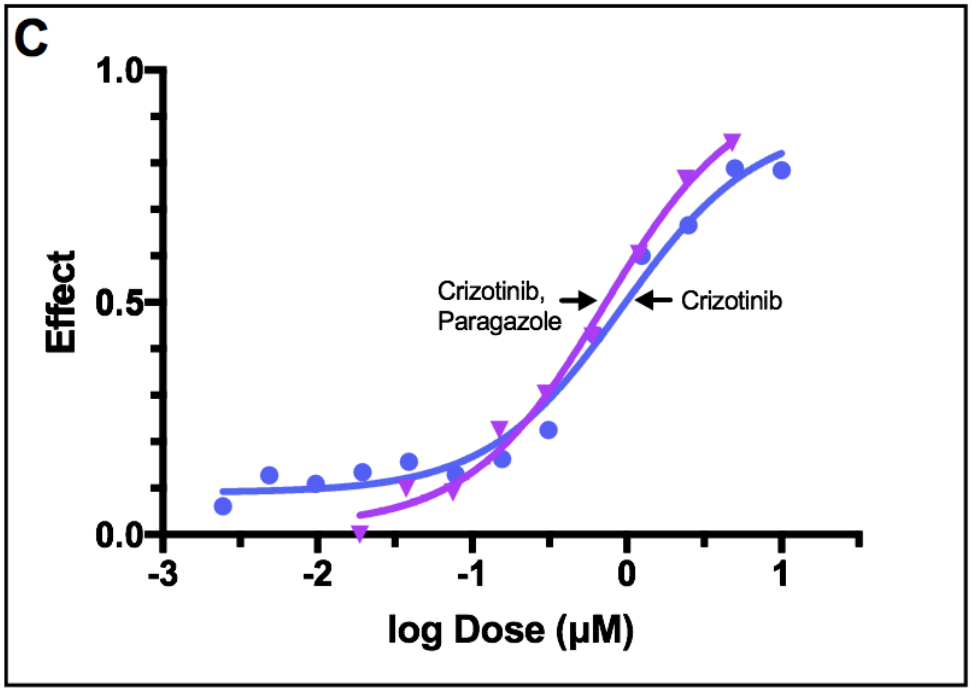
C
1.0
0.5
0.0
Effect
Crizotinib,
Paragazole
Crizotinib
-3
-2
-1
0
1
log Dose (μM)

.

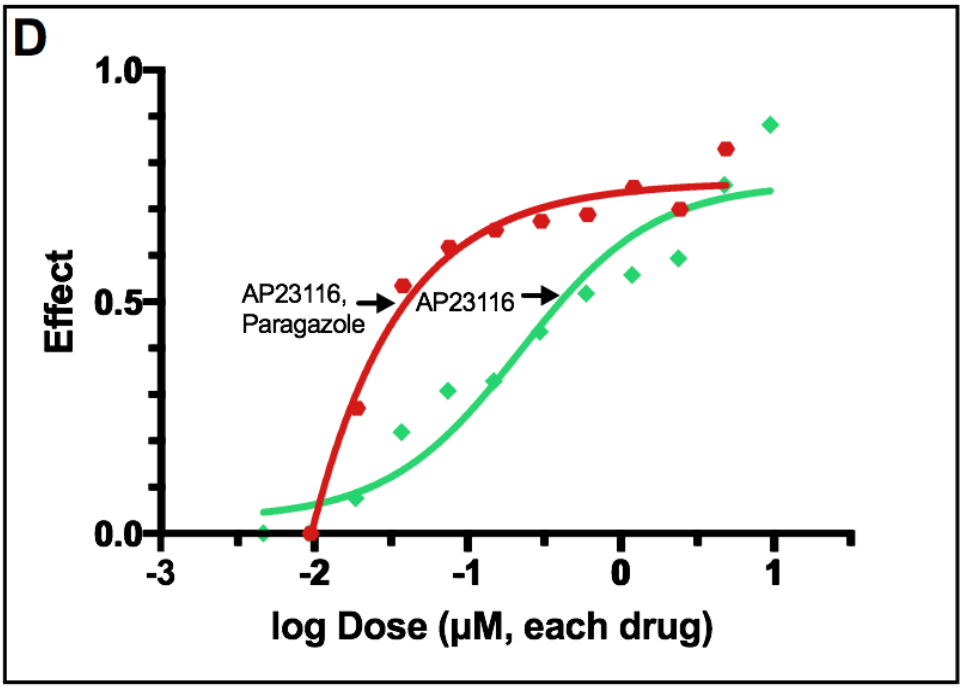
D
1.0
0.5
0.0
Effect
AP23116,
Paragazole
AP23116
-3
-2
-1
0
1
log Dose (μM, each drug)

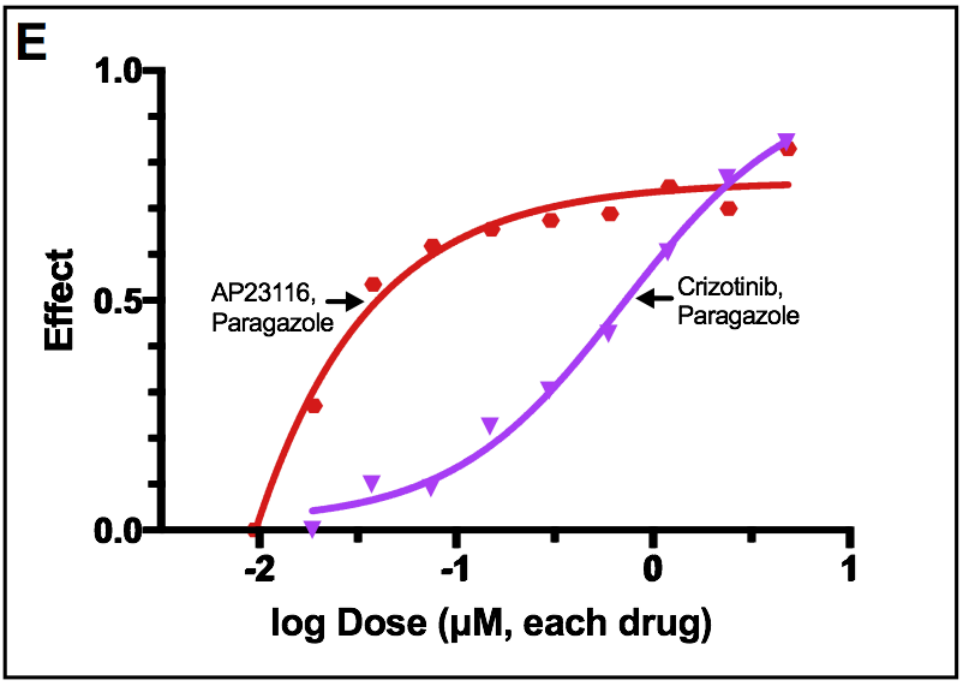
E
1.0
0.5
0.0
Effect
AP23116,
Paragazole
Crizotinib,
Paragazole
-2
-1
0
1
log Dose (μM, each drug)

Staggered Combination Treatments

Since synergistic activity was observed with each ALKi/HDACi combination, staggered combination experiments were conducted in order to establish if the observed effects were dependent on ALKi or HDACi. These experiments were done by initially treating H3122s with one drug, followed by the addition of the other drug of the pair after 24 hours. Both combinations yielded stronger responses when ALKi was the initial treatment. As expected, due to the difference in potency between the two ALK inhibitors, the initial addition of AP23116 exhibited higher potency and biological activity (*Fig. 6B)* compared to when crizotinib was the initial treatment (*Fig. 6A)*. Also, as expected, a higher potency was achieved when AP23116 was the secondary treatment compared to crizotinib. Due to the fact that survival of ALK+ cancers is highly dependent on constitutive ALK activation, it is not surprising that ALK inhibition appears to be the dominating factor. However, the discrepancy between responses of ALKi as initial vs. secondary treatment could be due to the large difference in potency between both ALK inhibitors and paragazole. Judging by the relatively low efficacy of paragazole single-drug treatment, it would not be expected that HDAC inhibition would lend itself to greater ALKi effectiveness, yet simultaneous combination treatment yields dramatic results. In order to truly determine whether or not the observed synergistic activity is HDAC- or ALK-dependent, comprehensive mechanistic studies would be have to be conducted.

Figure 6. *Staggered combination treatments; dosage represents the concentration of each drug in combination. (1) denotes initial treatment, while (2) denotes secondary treatment after 24 hours.*

(A) Overlay of dose-responses of crizotinib & paragazole in combination.

(B) Overlay of dose-responses of AP23116 & paragazole in combination

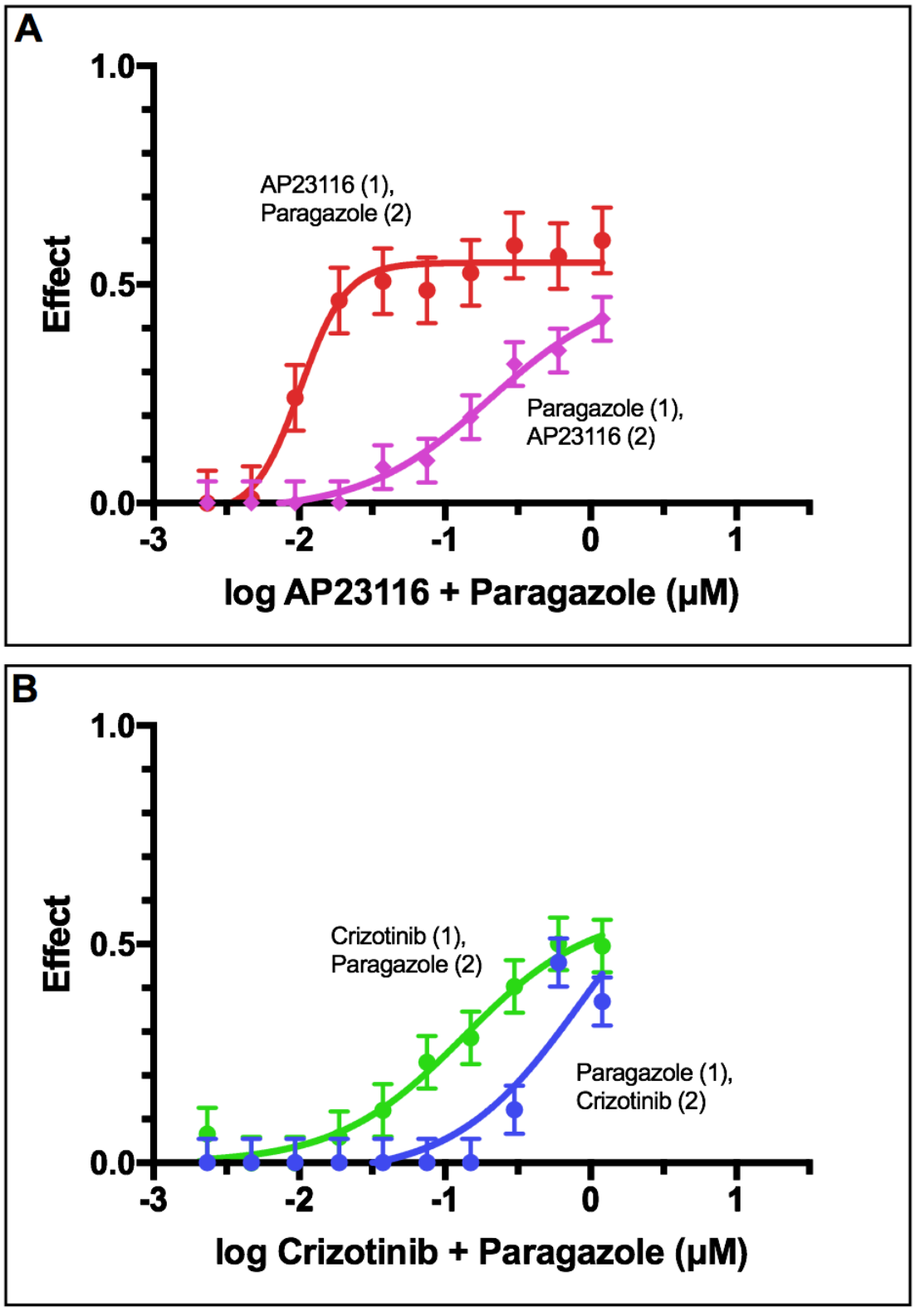

Discussion

Combination therapy is becoming a widely used strategy to more efficaciously treat patients diagnosed with cancers harboring genetic aberration, specifically those which confer drug resistance. Approximately 70,000 people are diagnosed with ALK-EML4-positive non-small cell lung cancer each year (Sasaki et al. 2010). The prevalence of these diagnoses necessitates the formulation of effective, specialized treatments that can overcome the resistance mechanisms of the ALK-EML4 gene fusion. While tyrosine kinase inhibitors (TKI) continue to be used in clinical trials to treat these patients to inhibit the kinase activity of the fusion product, acquired drug resistance to ALK inhibition therapy is nearly inevitable. Therapeutic combinations are a promising method to overcome resistance mechanisms such as ALK gene amplification and point mutations in the ALK kinase domain. In this project, it was found that combining of ALK inhibitors (crizotinib or AP23116) with the HDAC inhibitor, paragazole, produces synergistic effects that are considerably more effective than any of the three single-drug treatments. While the AP23116/paragazole combination was found to be more potent than crizotinib/paragazole, this confirms that combined ALK and HDAC inhibition is a valid potential therapeutic approach to treating ALK-EML4 cancers. Definitively inducing cell death in ALK-EML4 tumors would prevent acquired drug resistance from occurring in wild-type cells and inhibit survival of those with resistance-related mutations.

From a mechanistic perspective, there are numerous studies that rationalize the synergistic effects of combined ALK and HDAC inhibition. Many selective TKIs have been found to effectively induce apoptosis in ALK-EML4 NSCLC. ALK inhibition induces expression of key pro-apoptotic factors and represses pro-survival factors by markedly abrogating phosphorylation of ALK, ERK, and STAT3 (Katayama et al. 2012; Takezawa et al.

2011). ALK inhibitors such as crizotinib and AP23116, among many others, have known therapeutic value, and understandably so since ALK-EML4 cells rely on constitutive ALK activation for survival and proliferation. So why does class-I HDAC inhibition, a less powerful treatment, yield ALK-EML4 lung cancer that much more sensitive to ALKi therapy? The key may be that these cancers greatly rely upon HDAC activity on both histone and non-histone substrates to survive, in addition to ALK activation. HDAC expression has been implicated with mediating tumor progression in a variety of cancers (Damaskos et al. 2018). Furthermore, a variety of HDAC inhibitors, including quisinostat and trichostatin A (TSA), have been found to induce both intrinsic and extrinsic apoptotic pathways in various lung cancers (Miyanaga et al. 2008). It has been reported that HDACi activates extrinsic death receptor pathways, such as tumor necrosis factor (TNF), by up-regulating various TNF receptors as well as their ligands at the transcriptional level (Zhang et al. 2014). HDACi has also been shown to induce intrinsic apoptotic pathways via p53 activation. By inactivating nuclear histone deacetylases, p53 becomes hyperacetylated, preventing its inactivation via ubiquitination by MDM2 (Zhuang 2013). p53 activation induces expression of many downstream pro-apoptotic factors of the Bcl-2 family, such as Bim. Zhang et al. reports that transcriptional activation of pro-apoptotic Bcl-2 factors is also mediated by hyperacetylation of the H3 and H4 histone subunits, a result of class-I HDAC inhibition. Bao et al. also observed this hyperacetylation of H3 and H4 as a result of quisinostat treatment. Finally, HDAC inhibition has been shown to abrogate STAT3 activity, an essential transcriptional regulator of factors that promote cell survival, growth, proliferation, and differentiation (Takezawa et al. 2011). Hyperacetylation of STAT3 due to HDACi has been shown to inhibit its phosphorylation and catalyze its translocation from

the nucleus to the cytoplasm, therefore diminishing its capability to induce transcription of its downstream factors (Gupta et al. 2009; Zhuang 2013).

The fact that both ALKi and HDACi produce overlapping and non-overlapping effects in terms of stimulating pro-apoptotic pathways could very well explain the synergistic relationship between the two inhibitors when administered to ALK-EML4 cancers. When combined with depletion of ALK and STAT3 activity via ALKi, concurrent activation of the TNF pathway, along with the up-regulation of pro-apoptotic Bcl-2 proteins via p53 induction and histone hyperacetylation, HDACi may overcome pro-survival mechanisms utilized by ALK-EML4 NSCLCs. Certainly a threshold is reached wherein the pro-apoptotic effects of ALK and HDAC inhibition overcome all pro-survival pathways and induce cell death. While much mechanistic-focused work must be done to validate this hypothesis, recent research, as well as the data presented in this paper, confirms the legitimacy of combining ALKi with HDACi as a means of treating ALK-EML4 cancers. In addition to establishing the precise mechanisms that confer synergy between these two drugs, employing this combination therapy on ALK-EML4 cells that exhibit ALKi-resistance would further the validity and value of this particular approach. Only by formulating a specialized treatment that is capable of overcoming acquired drug resistance to ALKi therapy can we improve the quality and longevity of life of those diagnosed with ALK-EML4-positive cancers.

References

Bao, Lianmin, Hua Diao, Nian Dong, Xiaoqiong Su, Bingbin Wang, Qiongya Mo, Heguo Yu, Xiangdong Wang, and Chengshui Chen. "Histone Deacetylase Inhibitor Induces Cell Apoptosis and Cycle Arrest in Lung Cancer Cells via Mitochondrial Injury and P53 Up-Acetylation." *Cell Biology and Toxicology* 32, no. 6 (December 1, 2016): 469–82.

Bayliss, Richard, Jene Choi, Dean A. Fennell, Andrew M. Fry, and Mark W. Richards. "Molecular Mechanisms That Underpin EML4-ALK Driven Cancers and Their Response to Targeted Drugs." *Cellular and Molecular Life Sciences* 73 (2016): 1209–24.

Chia, Puey Ling, Paul Mitchell, Alexander Dobrovic, and Thomas John. "Prevalence and Natural History of ALK Positive Non-Small-Cell Lung Cancer and the Clinical Impact of Targeted Therapy with ALK Inhibitors." *Clinical Epidemiology* 6 (November 20, 2014): 423–32.

Chiarle, Roberto, Claudia Voena, Chiara Ambrogio, Roberto Piva, and Giorgio Inghirami. "The Anaplastic Lymphoma Kinase in the Pathogenesis of Cancer." *Nature Reviews Cancer* 8, no. 1 (January 2008): 11–23.

Damaskos, Christos, Ioannis Tomos, Nikolaos Garmpis, Anna Karakatsani, Dimitrios Dimitroulis, Anna Garmpi, Eleftherios Spartalis, et al. "Histone Deacetylase Inhibitors as a Novel Targeted Therapy Against Non-Small Cell Lung Cancer: Where Are We Now and What Should We Expect?" *Anticancer Research* 38, no. 1 (January 1, 2018): 37–43.

Gupta, Mamta, Mary Stenson, Terra Lasho, Ayalew Tefferi, Anne Novak, Stephen M. Ansell, and Thomas E. Witzig. "Interplay Between Histone Deacetylases (HDACs) and STAT3: Mechanism of Activated JAK/STAT3 Oncogenic Pathway in ABC (Activated B-Cell) Type Diffuse Large B Cell Lymphoma." *Blood* 114, no. 22 (November 20, 2009): 925–925.

Heuckmann, Johannes M., Hyatt Balke-Want, Florian Malchers, Martin Peifer, Martin L. Sos, Mirjam Koker, Lydia Meder, et al. "Differential Protein Stability and ALK Inhibitor Sensitivity of EML4-ALK Fusion Variants." *Clinical Cancer Research* 18, no. 17 (September 1, 2012): 4682–90.

Katayama, Ryohei, Tahsin M. Khan, Cyril Benes, Eugene Lifshits, Hiromichi Ebi, Victor M. Rivera, William C. Shakespeare, A. John Iafrate, Jeffrey A. Engelman, and Alice T. Shaw. "Therapeutic Strategies to Overcome Crizotinib Resistance in Non-Small Cell Lung Cancers Harboring the Fusion Oncogene EML4-ALK." *Proceedings of the National Academy of Sciences of the United States of America* 108, no. 18 (May 3, 2011): 7535–40.

Katayama, Ryohei, Alice T. Shaw, Tahsin M. Khan, Mari Mino-Kenudson, Benjamin J. Solomon, Balazs Halmos, Nicholas A. Jessop, et al. "Mechanisms of Acquired Crizotinib Resistance in ALK-Rearranged Lung Cancers." *Science Translational Medicine* 4, no. 120 (February 8, 2012): 120ra17-120ra17.

Li, Yongjun, Xiaofen Ye, Jinfeng Liu, Jiping Zha, and Lin Pei. "Evaluation of EML4-ALK Fusion Proteins in Non-Small Cell Lung Cancer Using Small Molecule Inhibitors." *Neoplasia (New York, N.Y.)* 13, no. 1 (January 2011): 1–11.

Miyanaga, Akihiko, Akihiko Gemma, Rintaro Noro, Kiyoko Kataoka, Kuniko Matsuda, Michiya Nara, Tetsuya Okano, et al. "Antitumor Activity of Histone Deacetylase Inhibitors in Non-Small Cell Lung Cancer Cells: Development of a Molecular Predictive Model." *Molecular Cancer Therapeutics* 7, no. 7 (July 1, 2008): 1923–30.

Sang, Jim, Jaime Acquaviva, Julie C. Friedland, Donald L. Smith, Manuel Sequeira, Chaohua Zhang, Qin Jiang, et al. "Targeted Inhibition of the Molecular Chaperone Hsp90 Overcomes ALK Inhibitor Resistance in Non-Small Cell Lung Cancer." *Cancer Discovery* 3, no. 4 (April 2013): 430–43.

Sasaki, Takaaki, Scott J. Rodig, Lucian R. Chirieac, and Pasi A. Jänne. "The Biology and Treatment of EML4-ALK Non-Small Cell Lung Cancer." *European Journal of Cancer (Oxford, England : 1990)* 46, no. 10 (July 2010): 1773–80.

Soda, Manabu, Young Lim Choi, Munehiro Enomoto, Shuji Takada, Yoshihiro Yamashita, Shunpei Ishikawa, Shin-ichiro Fujiwara, et al. "Identification of the Transforming EML4–ALK Fusion Gene in Non-Small-Cell Lung Cancer." *Nature* 448, no. 7153 (August 2, 2007): 561–66.

Takezawa, Ken, Isamu Okamoto, Kazuto Nishio, Pasi A. Jänne, and Kazuhiko Nakagawa. "Role of ERK-BIM and STAT3-Survivin Signaling Pathways in ALK Inhibitor–Induced Apoptosis in EML4-ALK–Positive Lung Cancer." *Clinical Cancer Research* 17, no. 8 (April 15, 2011): 2140–48.

Twarog, Nathaniel R., Elizabeth Stewart, Courtney Vowell Hammill, and Anang A. Shelat. "BRAID: A Unifying Paradigm for the Analysis of Combined Drug Action." *Scientific Reports* 6 (May 10, 2016): 25523.

Wang, Hui Qin, Ensar Halilovic, Xiaoyan Li, Jinsheng Liang, Yichen Cao, Daniel P Rakiec, David A Ruddy, et al. "Combined ALK and MDM2 Inhibition Increases Antitumor Activity and Overcomes Resistance in Human ALK Mutant Neuroblastoma Cell Lines and Xenograft Models." *ELife* 6. Accessed September 18, 2017.

Yoshida, Tatsuya, Yuko Oya, Kosuke Tanaka, Junichi Shimizu, Yoshitsugu Horio, Hiroaki Kuroda, Yukinori Sakao, Toyoaki Hida, and Yasushi Yatabe. "Differential Crizotinib Response Duration Among ALK Fusion Variants in ALK-Positive Non–Small-Cell Lung Cancer." *Journal of Clinical Oncology* 34, no. 28 (September 27, 2016): 3383–89.

Zhang, Jing, and Qing Zhong. "Histone Deacetylase Inhibitors and Cell Death." *Cellular and Molecular Life Sciences : CMLS* 71, no. 20 (October 2014): 3885–3901.

Zhuang, Shougang. "Regulation of STAT Signaling by Acetylation." *Cellular Signalling* 25, no. 9 (September 2013): 1924–31.